ENHANCED PROPORTIONAL-DERIVATIVE CONTROL OF A MICRO QUADCOPTER

Norman L. Johnson and Kam K. Leang*
Department of Mechanical Engineering
University of Nevada, Reno
Reno, Nevada 89557-0312, USA

ABSTRACT

This paper studies the design of an enhanced proportional-derivative (PD) controller to improve the transient response of a micro quadrotor helicopter (quadcopter). In particular, the controller minimizes the effect of disturbances by considering the orientation and rotation of the platform. A dynamics model is developed for an experimental micro quadcopter platform, and simulation results are presented that compare the proposed enhanced PD controller to a standard PD controller. Results show a 50% reduction in the peak response and a 45% reduction in the settling time, demonstrating the effectiveness of the controller.

1 Introduction

Micro aerial vehicles (MAVs) have a wingspan less than 0.15 m and a mass less than 0.1 kg [1]. Recent advances in technology have enabled the development of high-performance MAVs and currently MAVs include fixed wing aircraft, flapping wing aircraft, coaxial helicopters, trirotor helicopters, and quadrotor helicopters [2]. These small vehicles are well suited for applications which include autonomous sensor networks for remotely detecting environmental hazards, and surveillance, search, and rescue operations in areas that are dangerous to humans. For high-performance operation, an enhanced proportional-derivative (PD) controller posed in quaternion space which takes into account the actual rotational behavior of the MAV is proposed. Such a controller, compared to a standard PD controller, offers improved transient response. The experimental system is shown in Fig. 1, and the system is modeled and characterized for controller design. Simulations are presented to demonstrate the controller's effectiveness.

The control of quadcopters has mostly been focused on maneuvering at near hover conditions. Several groups have performed aggressive, high speed maneuvers [3], however the work has been applied to systems larger than MAVs. Quadcopter control approaches include iterative learning control [3], linear quadratic regulator [5], sliding mode control, model predictive control [6], and variations of PID control [7]. While these controllers have been successfully implemented, limited work has been done on micro quadcopters. One of the main challenges is due to their small size, micro quadcopters are more susceptible to disturbances such as wind gusts making it difficult to do even the basic maneuver of hovering.

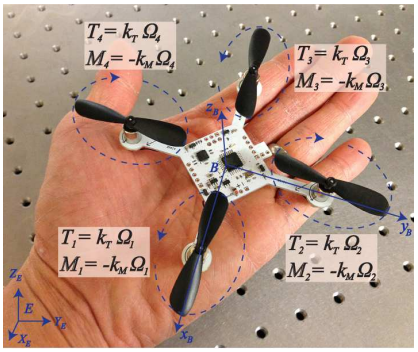

Figure 1. Experimental micro quadcopter platform, consisting of four in-plane motors and an on-board flight control system. The inertial reference frame, E, body reference frame, b, the direction of the rotor speed, Ω_i, and the applied forces, T_i, and moments, M_i with their accompanying equations shown in the figure. The constants k_T and k_M are the thrust constant and moment constant, respectively.

One of the main contributions of this work is the development of an enhanced PD control system for micro quadcopters that offer improved performance compared to a standard PD controller. In particular, the proposed enhanced PD controller min-

*Corresponding author; Email: kam@unr.edu; Phone/Fax: +1.775.784.7782/1701.

imizes the effect of disturbances by exploiting the principles of quaternion rotation. It is pointed out that the majority of the control systems are based on dynamic models which utilize Euler angles to describe the orientation of a vehicle. One problem with Euler angles is gimbal lock can occur causing singularities in calculations involving the rotation of the platform. Gimbal lock can be avoided by describing the rotation of the quadcopter using a unit quaternion [8]. In real world applications disturbances cause the quadcopter to rotate with some velocity. To minimize the effect of disturbances the enhanced PD controller defines the desired rotational velocity as a velocity that counteracts the rotational velocity caused by the disturbance. The controller is based off a PD control structure. However, compared to existing work which assumes that the desired rotation is zero [9], the error term in the rotational velocity is replaced with the measured rotational velocity. Thus, the proposed enhanced PD controller does not assume the desired rotational velocity is zero. Instead, it depends on a velocity that drives the system back to the original state.

2 The Experimental System and Modeling

2.1 The Experimental Quadcopter

The experimental micro quadcopter system (Mini Micro ARF Quadcopter) is shown in Fig. 1 and the system has a footprint of 68 mm by 68 mm. The body of the quadcopter is fabricated from a single printed circuit board, with integrated components that include a microcontroller (ATMEGA328P), three-axis gyro, accelerometer, and radio receiver. To minimize weight, the system is propelled by brushed DC motors. Compared to traditional designs where brushless motors are commonly used, brushed motors do not require sophisticated electronic speed controllers, thus reducing weight. However, the trade off in this case is longevity as brushed motors tend to wear more quickly during use compared to brushless motors. The entire system, which includes a battery (1S lithium battery), weighs 27.7 grams. Such a small and lightweight system has several advantages such as being maneuverable and agile. However, being small is more easily affected by external disturbances such as wind gusts.

2.2 Dynamic Model

The motion of a quadcopter consists of two components: the rotational motion and the translational motion, and, as shown in Fig. 1, is described in both the inertial reference frame E, defined by the coordinate system (X_E, Y_E, Z_E) and the quadcopter body frame b, defined by the coordinate system (x_b, y_b, z_b). The rotational motion describes the orientation and rotation of the quadcopter relative to the body frame. The rotation in the body frame is then transformed to rotation in the inertial frame. Rotation about the X_E-axis (roll) is defined by the angle ϕ, rotation about the Y_E-axis (pitch) is defined by the angle θ, and rotation about Z_E-axis (yaw) is defined by the angle ψ. On the other hand, the translational motion describes the position of the mass center of the vehicle and is relative to the inertial coordinate system. Finally, gravity acts in the negative Z_E-direction.

The quadcopter's position and attitude are affected by the thrust and moment generated by the four rotors. The thrust and moment caused by a single rotor are defined by

$$T_i = k_T \Omega_i^2, \quad M_i = -k_M \Omega_i^2, \tag{1}$$

where Ω_i is the angular velocity of the rotor with units of rpm, k_T is the thrust constant with units of $N/(rpm)^2$, and k_M is the moment constant with units of $m \cdot N/(rpm)^2$ [2]. When hovering, the force caused by the sum of the thrust vectors in the positive Z_E-direction is equal to the gravitational force, so $mg = (\Sigma T_i)_{Z_E}$, where T_i is the thrust caused by the i^{th} rotor. The speed of the i^{th} rotor is denoted by Ω_i. The roll angle of the quadcopter is adjusted by changing the thrust, T_2, with respect to the thrust, T_4, and the pitch angle of the quadcopter is adjusted by changing the thrust, T_1, with respect to the thrust, T_3. Yaw is controlled by the speed of the rotors. Each rotor causes a moment when it is rotating. For a quadcopter this moment can be negated by having two of the rotors spin counter to the other two. Thus, the yaw can be adjusted by changing the speed of the rotors. In this case, rotors 1 and 3 are spinning counter-clockwise and rotors 2 and 4 are spinning clockwise. The translational motion is derived in the inertial frame; however, the thrust from the rotors and drag acting on the body are described in the body frame and need to be transformed from the body frame to the inertial frame. Throughout this paper, vectors arrays are denote by $(\vec{\ })$ and quaternion arrays are in bold. Array subscript describes the reference frame. For scalars, the first subscript describes the reference frame and the second either describes the axis or rotor location as shown in Fig. 1.

2.2.1 Quaternions Quaternions are a method of representing 3-dimensional orientation using scalar and complex numbers. Each quaternion consists of four components and is described by $\mathbf{q} = [q_0, \vec{q}]$, where $\vec{q} = [q_1\mathbf{i}, q_2\mathbf{j}, q_3\mathbf{k}]^T$. The scalar q_0 represents the rotation about the axis defined by the unit vector $\vec{q}/|\vec{q}|$. Any position, velocity, and acceleration vector can be written in quaternion space by simply using the same components with no rotation. For example, the rotational velocity can be defined as $\omega_b = [0, \omega_{b,x}\mathbf{i}, \omega_{b,y}\mathbf{j}, \omega_{b,z}\mathbf{k}]^T$ and the thrust can be described as $\mathbf{T}_b = [0, 0, 0, \Sigma T_i \mathbf{k}]_b^T$.

The transformation from one frame to another is done by performing a quaternion product denoted by $\otimes$. The quaternion product between two quaternions, $\mathbf{p}$ and $\mathbf{q}$, is defined as $\mathbf{p} \otimes \mathbf{q} = [q_o p_o - \vec{q}^T \vec{p}, q_o \vec{p} + p_o \vec{q} + \vec{q} \times \vec{p}]^T$, and the product of two quaternions represents the sum of the two rotations. A general vector, $\mathbf{X}_b$ can be transformed from the body frame to the inertial frame by

$$\mathbf{X}_E = \mathbf{q} \otimes \mathbf{X}_b \otimes \mathbf{q}^*, \tag{2}$$

where $\mathbf{X} = [0, x_1\mathbf{i}, x_2\mathbf{j}, x_3\mathbf{k}]^T$ is some generic vector in quaternion space and $\mathbf{q}^*$ is the complex conjugate of the quaternion defined by $\mathbf{q}^* = \mathbf{q}^{-1} = [q_0, -q_1\mathbf{i}, -q_2\mathbf{j}, -q_3\mathbf{k}]^T$. For a rotating object, the change in orientation with respect to time can be found by

$$\dot{\mathbf{q}} = \frac{1}{2}\mathbf{q} \otimes \omega_b. \tag{3}$$

Equations (2) and (3) are used to transform between the body frame and the inertial frame. It is important to note that a singularity can occur during calculations of the rotational motion

since $\mathbf{q} = -\mathbf{q}$. This can be avoided by performing the calculations at small enough time intervals. Since it is more intuitive to view the objects attitude using Euler angles, one can find these by $\phi = \tan^{-1}\left[\frac{2(q_0q_1+q_2q_3)}{1-2(q_1^2+q_2^2)}\right]$, $\theta = \sin^{-1}[2(q_0q_2 - q_1q_3)]$, $\psi = \tan^{-1}\left[\frac{2(q_0q_3+q_1q_2)}{1-2(q_2^2+q_3^2)}\right]$.

Conversely, from the Euler angles the quaternion is:

$$q_0 = \cos(\phi/2)\cos(\theta/2)\cos(\psi/2) + \sin(\phi/2)\sin(\theta/2)\sin(\psi/2),$$
$$q_1 = \sin(\phi/2)\cos(\theta/2)\cos(\psi/2) - \cos(\phi/2)\sin(\theta/2)\sin(\psi/2),$$
$$q_2 = \cos(\phi/2)\sin(\theta/2)\cos(\psi/2) + \sin(\phi/2)\cos(\theta/2)\sin(\psi/2),$$
$$q_3 = \cos(\phi/2)\cos(\theta/2)\sin(\psi/2) - \sin(\phi/2)\sin(\theta/2)\cos(\psi/2).$$

2.2.2 Rotational Motion The rotational motion of the quadcopter describes the angle and rotation of the vehicle as it is moving through its environment. The equations of rotational motion can be derived from Newton's Second Law

$$\overline{\overline{I}}_b \dot{\vec{\omega}}_b = \Sigma \vec{M}_b, \tag{4}$$

where $\overline{\overline{I}}_b$, $\dot{\vec{\omega}}_b$ and $\vec{M}_b$ are the inertia matrix, rotational acceleration in the body frame and the sum of the moments about the center of mass, respectively. Due to the symmetry of the quadcopter, the moment of inertia of the system about the center of mass, $\overline{\overline{I}}_b$, is a diagonal matrix where $I_{b,11} = I_{b,22} = I_{b,xx} = I_{b,yy}$ and $I_{b,33} = I_{b,zz}$. The rotational acceleration, $\dot{\vec{\omega}}_b$, is described in the body frame by the vector $[\dot{\omega}_{b,x}, \dot{\omega}_{b,y}, \dot{\omega}_{b,z}]^T$. Similarly, the rotational velocity, $\vec{\omega}_b$ is the velocity at which the quadcopter rotates in the body frame and is described by the vector $[\omega_{b,x}, \omega_{b,y}, \omega_{b,z}]^T$. The sum of the moments about the center of gravity is described by the vector $[M_{b,x}, M_{b,y}, M_{b,z}]^T$ and is derived as follows.

The moments acting at the center of gravity of the body are

$$\begin{aligned}\Sigma \vec{M}_b = \Sigma \vec{M}_T - \vec{\omega}_b \times \overline{\overline{I}}_b \vec{\omega}_b \\ - J_r \vec{\omega}_b \times [0,\, 0\,, (-\Omega_1 + \Omega_2 - \Omega_3 + \Omega_4)]^T,\end{aligned} \tag{5}$$

where J_r is a scalar representing the inertia of a single rotor and Ω_i is the speed of the i^{th} rotor (see Fig. 1). Additionally, $\Sigma \vec{M}_T$ is the vector representing the moments caused by the rotors along the x-axis, y-axis and z-axis, $\vec{\omega}_b \times \overline{\overline{I}}_b \vec{\omega}_b$ is the gyroscopic torque caused by the rotation of the platform and $J_r \vec{\omega}_b \times [0,\, 0\,, (-\Omega_1 + \Omega_2 - \Omega_3 + \Omega_4)]^T$ is the gyroscopic torque caused by the rotation of the rotors. The sum of the moments, $\Sigma \vec{M}_T$, is derived by inspecting the moments acting on the platform. For the quadcopter, these forces act along the z_b-axis; therefore the pitch and roll are caused by the moments

$$\begin{aligned}\Sigma M_{b,x} = L_2 T_2 - L_4 T_4 - \omega_{b,y}\omega_{b,z}(I_3 - I_2) \\ - J_r \dot{\omega}_{b,y}(-\Omega_1 + \Omega_2 - \Omega_3 + \Omega_4),\end{aligned} \tag{6}$$

$$\begin{aligned}\Sigma M_{b,y} = L_1 T_1 - L_3 T_3 - \omega_{b,x}\omega_{b,z}(I_1 - I_3) \\ + J_r \dot{\omega}_{b,x}(-\Omega_1 + \Omega_2 - \Omega_3 + \Omega_4),\end{aligned} \tag{7}$$

where L_i is the length from the center of mass to the i^{th} rotor, and T_i is the thrust of the i^{th} rotor. In Eq. (6) and (7), $L_i T_i$ is the moment caused by the thrust of the i^{th} rotor. Substituting Eq. (1) into Eq. (6) and Eq. (7) results in

$$\begin{aligned}\Sigma M_{b,x} = L_2 k_T (\Omega_2)^2 - L_4 k_T (\Omega_4)^2 - \omega_{b,y}\omega_{b,z}(I_3 - I_2) \\ - J_r \dot{\omega}_{b,y}(-\Omega_1 + \Omega_2 - \Omega_3 + \Omega_4),\end{aligned} \tag{8}$$

$$\begin{aligned}\Sigma M_{b,y} = L_1 k_T (\Omega_1)^2 - L_3 k_T (\Omega_3)^2 - \omega_{b,x}\omega_{b,z}(I_1 - I_3) \\ + J_r \dot{\omega}_{b,x}(-\Omega_1 + \Omega_2 - \Omega_3 + \Omega_4).\end{aligned} \tag{9}$$

Typically, the length from the center of mass to the rotor can be approximated as the same for each rotor so that $L = L_1 = L_2 = L_3 = L_4$. Finally, the moment around the z_b-axis is

$$\Sigma M_{b,z} = -k_M(-\Omega_1^2 + \Omega_2^2 - \Omega_3^2 + \Omega_4^2) - \omega_{b,x}\omega_{b,y}(I_2 - I_1). \tag{10}$$

These equations are used to describe the rotational motion of a quadcopter. The orientation of the vehicle directly affects the translational motion which is described next.

2.2.3 Translational Motion The translational equations of motion are derived from the thrust, the drag force, and the force of gravity. The translational motion equations are derived in quaternion space from Newton's Second Law and are

$$m\ddot{\mathbf{x}}_E = \mathbf{T}_b + \mathbf{D}_b + \mathbf{W}_E. \tag{11}$$

The thrust from the rotors is described by the vector, $\mathbf{T}_b = [0,\, 0,\, 0,\, \Sigma T_{b,i}]^T$, where ΣT_i is the sum of the thrust from each rotor. The drag force is also acting in the body frame and is described by the vector $\mathbf{D}_b = c[0, V_{b,x}, V_{b,y}, V_{b,z}]^T$. The gravitational force is described in the inertial frame by the vector $\mathbf{W}_E = [0,\, 0,\, 0,\, -mg]^T$, where mg is the weight of the aircraft. The acceleration, $\ddot{\mathbf{x}}_E$, is described by the vector $[0, \ddot{x}_{E,X}, \ddot{x}_{E,Y}, \ddot{x}_{E,Z}]^T$. To express the entire equation in the inertial frame, the sum of the thrust and the drag force are rotated using quaternions, that is

$$m\ddot{\mathbf{x}}_E = \mathbf{q} \otimes (\mathbf{T}_E + \mathbf{D}_b) \otimes \mathbf{q}^* + \mathbf{W}_E. \tag{12}$$

The equations of translational motion, combined with the equations of rotational motion, completely describe the motion of the quadcopter. Quaternions are used to describe forces in the inertial frame. The enhanced PD controller is built from this model of the quadcopter.

3 Enhanced PD Control

The enhanced PD controller minimizes disturbances to the quadcopter system by defining the desired rotation velocity as the necessary rotational velocity to counteract disturbances. The controller is based off a PD controller [9] defined by

$$\tau = k_p \mathbf{q}_e + k_d \omega_e, \tag{13}$$

where τ is the change in rotation needed to correct the error, $\mathbf{q}_e$ represents the difference between the desired attitude, $\mathbf{q}_d$, and the measured attitude of the quadcopter, $\mathbf{q}_m$, and ω_e represents the difference between the measured rotation of the vehicle, ω_m and the desired rotation of the vehicle, ω_d. The necessary rotor speed can be derived from τ by [4],

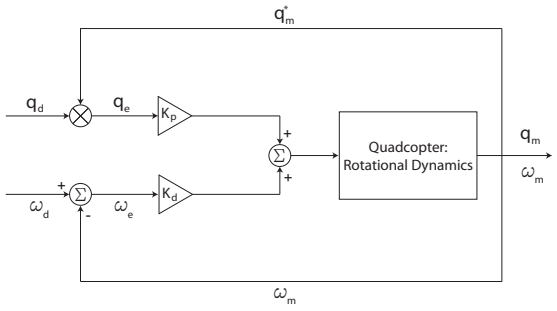

Figure 2. The enhanced PD control system. The error quaternion, $\mathbf{q}_e$, is defined as the quaternion product $\otimes$ of the conjugate of the measured quaternion, $\mathbf{q}_m^*$, and the desired quaternion, $\mathbf{q}_d$. The rotational velocity error, ω_e, is the difference between the desired rotational velocity, ω_d measured rotational velocity, ω_m.

$$\begin{bmatrix}\Omega_1\\ \Omega_2\\ \Omega_3\\ \Omega_4\end{bmatrix} = \begin{bmatrix}1 & 0 & 1 & 1\\ 1 & 1 & 0 & -1\\ 1 & 0 & -1 & 1\\ 1 & -1 & 0 & -1\end{bmatrix}\begin{bmatrix}\Omega_h\\ \tau(2)\\ \tau(3)\\ \tau(4)\end{bmatrix}, \tag{14}$$

where Ω_h is the rotor speed required to hover. The block diagram of the PD control system is shown in Fig. 2.

For most applications of Eq. (13), it is assumed that the desired rotation is zero so that ω_e is replaced by ω_m. The following controller instead uses quaternion principles discussed in Sec. 2.2.1 to derive ω_e. For this controller, the desired rotational velocity is some velocity that counteracts the measured rotational velocity. The derivation of ω_e uses the rules found in Eqs. (3), (15), and (16) for quaternion $\mathbf{q}$:

$$\mathbf{q}_d = \mathbf{q}_m \otimes \mathbf{q}_e, \tag{15}$$

$$\dot{\mathbf{q}}_d = \dot{\mathbf{q}}_m \otimes \mathbf{q}_e + \mathbf{q}_m \otimes \dot{\mathbf{q}}_e. \tag{16}$$

By solving Eq. (3) for ω_d and substituting Eq. (15) into Eq. (16), ω_d can be defined by

$$\omega_d = \mathbf{q}_d^* \otimes \mathbf{q}_m \otimes \omega_m \otimes \mathbf{q}_e + 2\mathbf{q}_d^* \otimes \mathbf{q}_m \otimes \dot{\mathbf{q}}_e. \tag{17}$$

The effect that the error quaternion, $\mathbf{q}_e$, has on performance of quadcopter can be controlled by

$$\omega_d = K_p\mathbf{q}_d^* \otimes \mathbf{q}_m \otimes \omega_m \otimes \mathbf{q}_e + K_d\mathbf{q}_d^* \otimes \mathbf{q}_m \otimes \dot{\mathbf{q}}_e, \tag{18}$$

where K_p and K_d dictate how much influence the error quaterion and its derivative, $\mathbf{q}_e$ and $\dot{\mathbf{q}}_e$ respectively, have on the system. Note that for no rotation $\mathbf{q}_e = [1, 0, 0, 0]^T$. Equation (18) can be used to define ω_e by $\omega_e = \omega_d - \omega_a$ so that

$$\omega_e = K_p\mathbf{q}_d^* \otimes \mathbf{q}_m \otimes \omega_m \otimes \mathbf{q}_e + K_d\mathbf{q}_d^* \otimes \mathbf{q}_m \otimes \dot{\mathbf{q}}_e - \omega_m. \tag{19}$$

Equation (21) can simplified further by substituting Eq. (17) and Eq. (5) for $\mathbf{q}_e$ and $\dot{\mathbf{q}}_e$ respectively and solving for ω_e so that

$$\omega_e = (\mathbf{1} + K_d\mathbf{1})(K_p\mathbf{q}_d^* \otimes \mathbf{q}_m \otimes \omega_m \otimes \mathbf{q}_e - \omega_m), \tag{20}$$

where $\mathbf{1} = [1,0,0,0]^T$ is a quaternion representing no rotation and in quaternion multiplication is comparable to multiplying a matrix by the identity matrix. The enhanced PD controller can be derived by simplifying Eq. (20), and substituting it into Eq. (13) so that the final solution is

$$\tau = k_p\mathbf{q}_m^* \otimes \mathbf{q}_d + k_d(K_p\mathbf{q}_d^* \otimes \mathbf{q}_m \otimes \omega_m \otimes \mathbf{q}_m^* \otimes \mathbf{q}_d - \omega_m). \tag{21}$$

Equation (21) is composed of either desired terms or measured terms. The three terms, k_p, k_d, and K_p can be tuned to optimize the performance of the system. The controller can now be implemented and the results are discussed in Sec. 4.2.

4 Simulations and Discussion

4.1 Characterization

The characterization of the platform consists of measuring the total mass of the system m, the moment arm for each rotor L_1, L_2, L_3, L_4, the rotor force constant k_T, the rotor moment constant k_M, the rotor inertia about the z-axis J_r, the moment of inertia about each axis I_x, I_y, I_z and calculating the drag coefficient of the platform c. The mass of the system was measured using a digital scale from Scalesco Measurement Technology Inc (model SMT-1008) with a resolution of 0.01 g. The distance from the center of gravity to each rotor was measured using calipers with a resolution of 10 μm. The inertia of the system was calculated from a CAD model created in Autodesk Inventor®. The drag coefficient of the platform is taken from the value for a square plate moving perpendicular to air flow. Finally, the force and moment constants were measured using a Nano17, 6-axis load cell from ATI Industrial Automation. The Nano17 can measure force in the z-direction with a resolution of 1.5 mN and it can measure torque in the z-direction with a resolution of 6.9 mN $\cdot$ mm. A diagram of the test setup is shown in Fig. 3 and the results of these tests are shown in Fig. 4. The parameters of the quadcopter used for simulation are: mass, $m = 27.7$ g; length of arm 1, 2, 3, 4, $L_1 = L_2 = L_3 = L_4 = 39.62$ mm; thrust constant, $k_f = 5.861 \times 10^{-11}$ N/rpm^2; moment constant, $k_m = 3.089 \times 10^{-13}$ m·N/rpm^2; rotor inertia, $J_r = 0.0023$ kg·m^2; body inertia, $I_{xx} = I_{yy} = 12 \times 10^{-6}$ kg·m^2 and $I_{zz} = 23 \times 10^{-6}$ kg·m^2, and drag constant, $c = 1.17$ N/(m/s).

4.2 Results and Discussion

Equation (13) is used to benchmark the performance of the enhanced PD controller. For both controllers the proportional gain is $k_p = 1793$ and the derivative gain is $k_d = 75.8$. An initial rotational velocity is used to simulate a disturbance. Figures 5 and 6 compare the enhanced PD controller to a standard PD controller presented in other work, [9]. The disturbance of $360°/s$ is used to show the effectiveness of the controller and that even under extreme conditions the system will settle back to the original state in less than a second. In both cases the enhanced PD controller has a 45% decrease in the peak response and a 50% decrease in the settling time when compared to the benchmark controller. Additionally, the enhanced PD controller settles back to the nominal configuration without any overshoot.

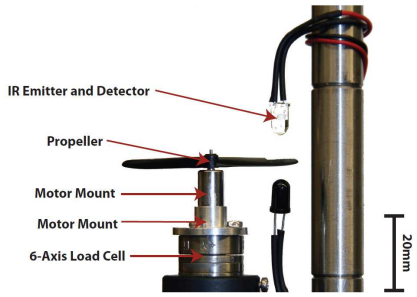

Figure 3. The test setup used to experimentally find the thrust and motor constants. The motor and rotor are mounted on a Nano17 6-axis sensor. An IR emitter and IR reciever were used to measure the rotor speed.

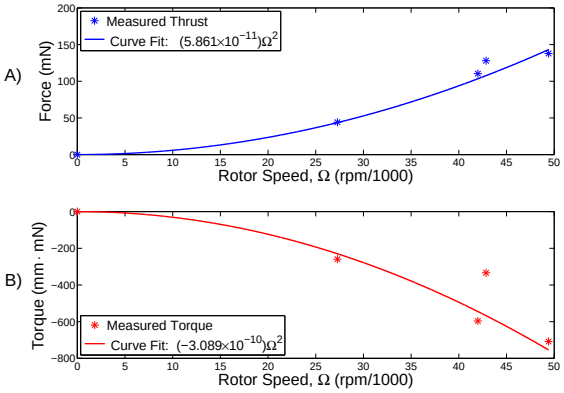

Figure 4. Characterization results: (a) force as a function of rotor speed and (b) moment caused by the rotor as a function of rotor speed.

5 Conclusions

The characterization and control of a micro quadcopter have been presented. Simulation results were presented to show the performance of the control system. When compared to a benchmark controller, the peak response of the system is decreased by 45% and the settling time is improved by 50%. In simulation, the enhanced PD controller effectively handles disturbances up to $360^\circ/s$. Future work includes an analysis of the stability of the controller and experimental verification of the proposed control scheme.

REFERENCES

[1] Petricca L., Ohlckers P., and Grinde C., Micro-and Nano-air Vehicles: State of the Art, *Int. J. of Aero. Eng.*, 2011, 2011.

[2] Kumar V. and Michael N., Opportunities and Challenges with Autonomous Micro Aerial Vehicles, *The Int. J. of Robotics Research*, 31(11):1279–1291, 2012.

[3] Lupashin S. and D'Andrea R., Adaptive Fast Open-loop Maneuvers for Quadrocopters, *Auton. Robots*, 33(1-2):1–14, 2012.

[4] Mellinger D., Michael N., and Kumar V., Trajectory Generation and Control for Precise Aggressive Maneuvers with Quadrotors, *Int. J. Robotics Research*, 31(5):664–674, 2012.

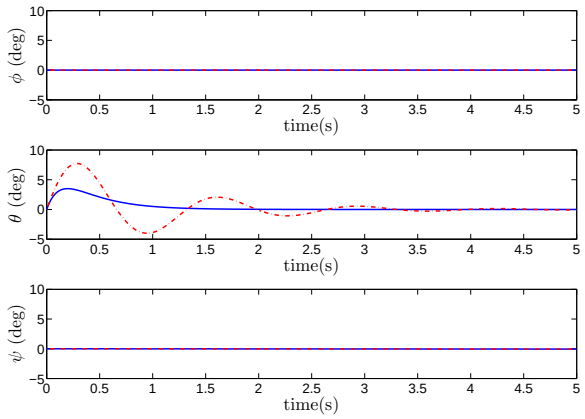

Figure 5. The enhanced PD controller (solid) is compared to a benchmark PD controller (dot-dash) for a disturbance of $50^\circ/s$ about the y-axis, θ. There is no disturbance about the *x*-axis, ϕ, or *z*-axis, ψ.

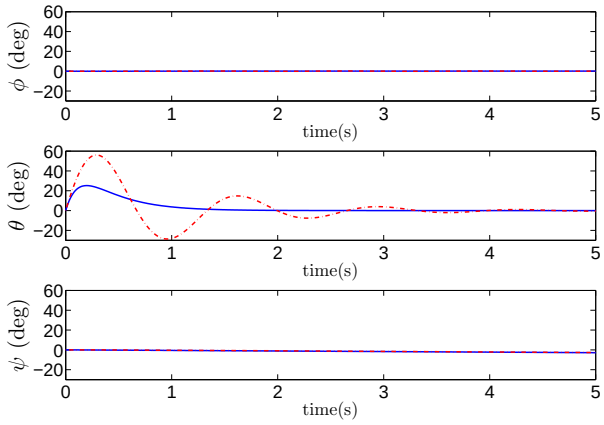

Figure 6. The enhanced PD controller (solid) is compared to a benchmark PD controller (dot-dash) for a disturbance of $360^\circ/s$ about the y-axis, θ and no disturbance about the *x*-axis, ϕ, or *z*-axis, ψ.

[5] Low B., Leongand S. and Ooi M., Low-cost Microcontroller-based Hover Control Design of a Quadcopter, *Procedia Engineering*, 41:458–464, 2012.

[6] Bouffard P., Aswani A., and Tomlin C., Learning-based model predictive control on a quadrotor: Onboard implementation and experimental results, In *IEEE Int. Conf. Robotics and Automation (ICRA)*, pp. 279–284, 2012.

[7] Tayebi A. and McGilvray S., Attitude stabilization of a VTOL quadrotor aircraft, *IEEE Trans. Cont. Sys. Tech.*, 14(3):562–571, 2006.

[8] Chou J., Quaternion Kinematic and Dynamic Differential Equations, *IEEE Trans. Robotics and Auto.*, 8(1):53–64, 1992.

[9] Caccavale F. and Villani L., Output Feedback Control for Attitude Tracking, *Systems & control letters*, 38(2):91–98, 1999.